The state of the union: air-sea interactions during coastal marine heatwaves

Robert W. Schlegel[a,*], Eric C. J. Oliver[b,c], Sarah Kirkpatrick[d], Andries Kruger[e,f], Albertus J. Smit[a]

[a]*Department of Biodiversity and Conservation Biology, University of the Western Cape, Private Bag X17, Bellville 7535, South Africa*
[b]*ARC Centre of Excellence for Climate System Science, Australia*
[c]*Institute for Marine and Antarctic Studies, University of Tasmania, Hobart, Australia*
[d]*UWA Oceans Institute and School of Plant Biology, The University of Western Australia, Crawley, 6009 Western Australia, Australia*
[e]*Climate Service, South African Weather Service, Pretoria, South Africa*
[f]*Department of Geography, Geoinformatics and Meteorology, Faculty of Natural and Agricultural Sciences, University of Pretoria, South Africa*

Abstract

The study and documentation of marine heatwaves (MHWs) is outpacing our understanding of the causes of these extreme climatic events. This is even more striking with regards to coastal MHWs. It is therefore becoming increasingly necessary to unravel the relationships between the potential physical drivers of an event and the event itself. An improved understanding of the mechanistic causal pathways of MHWs may allow us to better forecast the occurrence of these devastating events. To this end we have utilized oceanic (BRAN) and atmospheric (ERA-Interim) reanalysis data to examine the state of the air and sea around southern Africa during MHWs. Self-organising maps (SOMs) were then used to cluster each synoptic air-sea state during an event into 1 of 9 nodes to determine the predominant synoptic states during MHWs. It was found that abnormal ocean circulation forcing warm water onto the coast was the main cause of the recorded coastal MHWs. This abnormal circulation often work in tandem with abnormal wind. This may be taken as the first step of a more in depth exploratory analysis between what may be a causal link in the air-sea interaction at these mid-latitude locations.

Keywords: extreme events, air-sea interaction, reanalysis data, *in situ* data, climate change, nearshore

1. Introduction

Documentation on the negative impacts of changing climates due to anthropogenically forced warming on both marine and terrestrial ecosystems has grown rapidly over the last few decades. The primary focus of which tended towards the measuring of linear increases in mean temperatures in distinct regions. Whereas these long term changes are effecting a myriad of systems identified as critically important (Stocker et al., 2013), the major impacts on humans and ecosystems in the present are due to extreme events (Easterling et al., 2000). Often unpredictable, cyclones, floods, heatwaves and cold-spells may begin and end before any warning systems may be of use. It is for this reason, and

---

*Corresponding author
Email address:* `3503570@myuwc.ac.za` (Robert W. Schlegel)

others, that more of the focus within climate change research is now being applied to the study of
these extreme events (Jentsch et al., 2007).

Due to the currently sparse occurrence of such extreme events in time and space, very few have
impacted areas in which long term ecological data were being sampled *a priori*. Two well documented
exceptions to this trend are the long periods of aseasonally warm water that occurred in 2003 in
the Mediterranean and 2011 off the west coast of Australia. The 2003 Mediterranean event has been
documented to have negatively impacted as much as 80% of the Gorgonian fan colonies there (Garrabou
et al., 2009), whereas the 2011 Western Australia event is now known to have caused a permanent
100 km range contraction of the ecosystem forming kelp species *Ecklonia radiata* in favour of the
tropicalisation of reef fishes and seaweed turfs (Wernberg et al., 2016). Both of these anomalously
warm seawater temperature events are classified as 'marine heatwaves' (MHWs).

Various definitions for MHWs have been developed but it was Hobday et al. (2016) that created a
numeric definition of MHWs that allowed anomalously warm seawater temperature events occurring
anywhere on the globe to be directly comparable. Thus opening up the possibility of researching
common causes of these events through space and time. Whereas the common measurements created
for these events allowed for comparison, it still did not serve to answer what was causing these events.
Beyond common measurements, it is necessary to identify the possible range of physical causes of
MHWs so as to be able to compare similar 'types' of events and to be able to move towards a system
of prediction.

It is hypothesized that MHWs should either be caused by oceanic forcing, atmospheric forcing, or a
combination of the two. For example, the transport of warm water onto the coast of Western Australia
is responsible for the large scale MHW that occurred there in 2011 (Feng et al., 2013; Benthuysen
et al., 2014). However, recent research into the development of a mechanistic understanding between
local- *vs.* broad-scale influences on the formation of extreme events at coastal localities has revealed
that meso-scale forcing from offshore onto the nearshore (<400 m from the coast) is responsible for
the formation of MHWs far less than hypothesized (Schlegel and Smit, 2016). It is therefore necessary
to consider additional mechanisms or interactions that may be responsible for these events.

Air-sea interactions have been a focus of study for decades (Frankignoul, 1985), with mixed results.
Whereas interactions are often detectable at high latitudes, mid latitude relationships between air and
sea are much more tenuous (Krishnamurti et al., 1988). Equation 1 in Deser et al. (2010) shows the
process through which the upper mixed layer in the open ocean is effected by atmospheric and oceanic
process. Unfortunately this process does not appear to apply to the coastal regions of the world, of
which little is yet understood of the mechanistic processes driving the extreme events observed there.
In certain special instances, such as the 2003 heatwave over the Mediterranean described in Garrabou
et al. (2009) a clear connection may be drawn between the air and sea. This is however an exception
to the norm as most bodies of water are not subject to static atmospheric and oceanic conditions.
One reason given for the lack of apparent air-sea interactions at mid-latitudes is that the coupling of
these two media drives an increase in the variability of both, inhibiting heat flux from one to the other

(Barsugli and Battisti, 1998).

An earlier version of this manuscript sought to compare the co-occurrence of MHWs and atmospheric heatwaves (AHWs), both measured *in situ* along a coastline via the same methodology outlined in Schlegel and Smit (2016). The rates of co-occurrence for extreme events between these media were found to be lower than those found for nearshore and offshore seawater. It was therefore decided to create an index of mean synoptic air-sea states during the occurrence of coastal MHWs and then cluster them with the use of a self-organising map (SOM) to deduce the general patterns. The temperature dataset used for the calculation of the MHWs consisted of daily temperature records collected *in situ* at dozens of locations. The state of the sea, both SST and surface currents, were determined with the Bluelink ReANalysis (BRAN; wp.csiro.au/bluelink). The state of the air temperature and winds were determined with ERA-Interim (http://www.ecmwf.int/en/research/climate-reanalysis/era-interim). The aim of the clustering of the synoptic air-sea states from these datasets was to visualise broadscale patterns in the air and/ or sea that occur most regularly during MHWs at coastal localities. We hypothesized that i) similar air and sea mesoscale patterns would be revealed through clustering; ii) these patterns would be more distinct in the sea than the air; and iii) these observed similarities would aid in the development of a broader mechanistic understanding of the relationship between coastal MHWs and air-sea interactions.

2. Methods

2.1. Study region

The *ca.* 3,100 km long South African coast provides a natural laboratory for investigations into the offshore forcing of nearshore phenomena as it may be divided into three sections, allowing for a range of meso-scale influences to be considered within the same research framework (Figure 1). The entire west coast section of the country is distinct from the other two in that it is the realm of the Benguela Current, which forms an Eastern Boundary Upwelling System (EBUS) (Hutchings et al., 2009). Conversely, the east coast section is dominated by the Agulhas Current (Lünning, 1990), a poleward flowing current that transports warm water down from Madagascar. Trapped between these two mighty currents the south coast section is consistently tumultuous. More closely affiliated to the east coast than the west, the south coast nonetheless experiences both sheer forced and wind driven upwelling in addition to having significantly more thermal variability than either of the other two sections (Schlegel and Smit, 2016). The range of temperatures experienced along all three sections is large and the gradient of increasing temperature as one moves from the border of Namibia to the border of Mozambique is nearly linear. For a more detailed description of these sections see Smit et al. (2013).

2.2. In situ *data*

The coastal seawater temperature data used in this study were acquired from the South African Coastal Temperature Network (SACTN, https://github.com/ajsmit/SACTN, https://robert-schlegel.shinyapps.io/SACTN
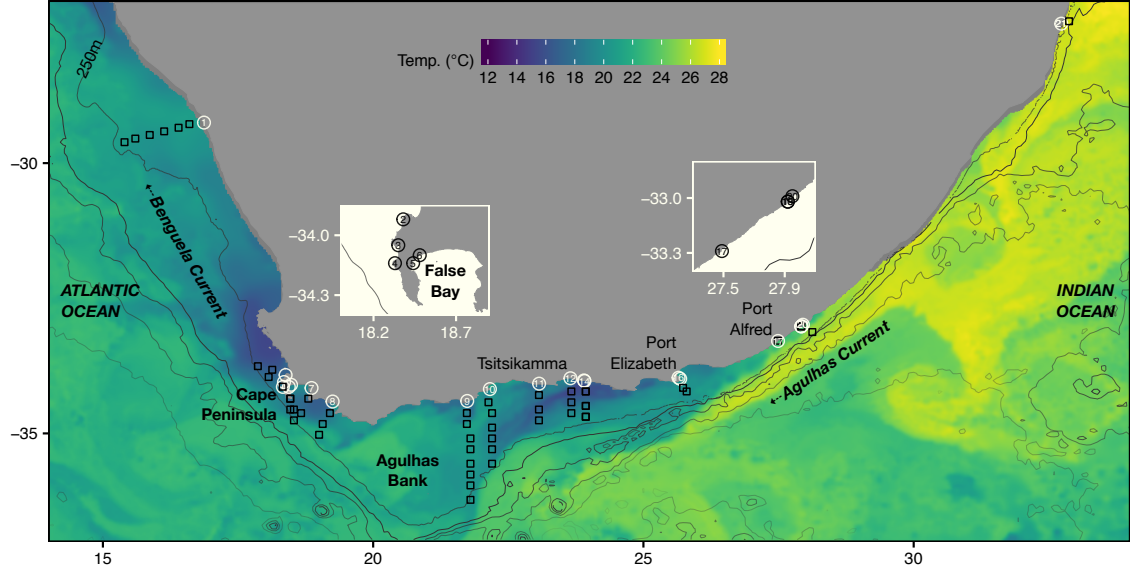
Figure 1: Map of southern Africa showing bathymetry and the location of the *in situ* temperature time series shown with circles. The inset maps show detail of the Cape Peninsula/ False Bay area and the Port Alfred region where site labels are obscured due to overplotting of symbols.

The SACTN data are contributed by seven different organizations and are collected *in situ* with a mixture of hand-held alcohol & mercury thermometers as well as digital underwater temperature recorders (UTRs). This data set currently consists of 135 daily time series, with a mean duration of 19.7 years. Therefore many of the time series in this dataset are shorter than the 30 year minimum proscribed for the characterization of MHWs (Hobday et al., 2016), with many having gaps of missing data above the recommended limit of 10%, too. It is however deemed necessary to use these data when investigating extreme events in the nearshore (<400 m from the low tide mark) as satellite derived sea surface temperature (SST) values along the coast have been shown to display large biases (Smit et al., 2013) or capture minimum and maximum temperatures poorly (Smale and Wernberg, 2009; Castillo and Lima, 2010). All of the *in situ* time series from the SACTN shorter than ten years or missing more than 10% of their daily temperature measurements were excluded from use in this study. This reduced the total time series to 26, with a mean length of 22.3 years. Table 3 shows the metadata for the SACTN time series used in this study.

2.3. Reanalysis data

To visualise a synoptic view of the air-sea state during marine heatwaves (MHWs) (see sections Marine heatwaves and Air-sea state below) it was necessary to use reanalysis products to provide air or sea temperatures with wind/ current vectors in a single product.

The 1/10°Bluelink ReAnalysis product was chosen to investigate the state of the sea around

southern Africa during coastal MHWs. This modelled product relies on the assimilation of an array of data collected *in situ* and remotely. This representation of the sea state is accurate on the scale of 10's of km or larger and is appropriate for the identification of meso-scale events. From this product were taken the sea surface temperature (SST) and surface currents for the study region. BRAN is available
105 for download via XML and is a product of the CSIRO (https://www.csiro.au/).

The state of the air was determined with the use of the ERA-Interim reanalysis product, which is produced by the European Centre for Medium-Range Weather Forecasts (ECMWF, http://www.ecmwf.int/). The native 3/4°resolution of this product is courser than BRAN however, it is available for download at finer resolution by interpolation of the data. The data used for this study were downloaded at a
110 resolution of 1/2°. The ERA-Interim variables used for this study were the surface temperature (2 m) and winds (10 m).

All variables from both reanalysis products were rounded to a resolution of 1/2°to ensure a numerically equal representation of the synoptic air and sea states. Once rounded the data were trimmed to contain the same longitude and latitude extents. All variables were then reprocessed into
115 the same data frame format for consistent analysis. The BRAN reanalysis product at the writing of this paper was available from January 1st, 1994 to August 31st, 2016. This is less than the range of data currently available for ERA-Interim at January 1st, 1979 to December 31st, 2016. All dates occurring outside of those in the BRAN product were excluded. The analysis period for the climatologies for the BRAN and ERA-Interim data are then January 1st, 1979 to December 31st, 2016.

120 *2.4. Marine heatwaves*

The term marine heatwave (MHW) as used here differs slightly from the definition of a heatwave originally developed for atmospheric events (Perkins and Alexander, 2013). Here we make use of the definition for marine heatwaves given in Hobday et al. (2016) as "a prolonged discrete anomalously warm water event that can be described by its duration, intensity, rate of evolution, and spatial extent."
125 The characterization of these events in this manner allows investigators from anywhere in the world to compare and classify events using common statistical properties. We therefore use the methodology laid out in Hobday et al. (2016) for the analysis of MHWs in this research.

The algorithm developed by Hobday et al. (2016) isolates MHWs by finding the days in which the temperature of a given locality exceeds the 90th percentile of temperatures found there, based on an
130 11-day moving average. Perkins and Alexander (2013) concluded that the minimum duration for the analysis of atmospheric heatwaves was 3 days. Hobday et al. (2016) found that a minimum length of 5 days allowed for more uniform global results in event detection, leading them to conclude that this would be a good default starting point for MHW detection. Previous work by Schlegel and Smit (2016) showed that the inclusion of these much shorter days led to spurious connections between events
135 found across different datasets. In this research we are interested in deducing the air-sea state patterns during very large MHWs. We found that eliminating events shorter than 15 days in length caused the removal 847 of the 976 total MHWs detected in the *in situ* dataset. The events that occurred before or after the reanalysis period were also excluded. This left us with 98 events over a 20 year period. It

5

Table 1: The descriptions for the metrics of MHWs as proposed by Hobday et al. (2016).

Name [unit]	Definition
Count [no. events per year]	n: number of MHWs per year
Duration [days]	D: Consecutive period of time that temperature exceeds the threshold
Maximum intensity [°C]	i_{max}: highest temperature anomaly value during the MHW
Mean intensity [°C]	i_{mean}: mean temperature anomaly during the MHW
Cumulative intensity [°C·days]	i_{cum}: sum of daily intensity anomalies over the duration of the event

must also be highlighted that any of the aforementioned 98 MHWs that had 'breaks' below the 90th percentile threshold lasting ≤2 days followed by subsequent days above the threshold were considered as one continuous event (Hobday et al., 2016).

In order to calculate a MHW it is necessary to supply a climatology against which daily values may be compared. It is proscribed in Hobday et al. (2016) that this period be at least 30 years. Because 20 of the 26 time series used here are below this threshold we have opted to use the first and last complete years of data for each individual time series as the climatological period against which the MHWs for each respective time series were calculated. By juxtaposing MHWs against daily climatologies, the amount they differ from their local standard may be quantified. The definitions for the metrics that will be focused on in this paper may be found in Table 1.

We calculated the MHWs in the SACTN dataset with the use of the R package 'RmarineHeatWaves', which may be downloaded via CRAN (https://cran.r-project.org/web/packages/RmarineHeatWaves/index.html), with the developmental version available on GitHub (https://github.com/ajsmit/RmarineHeatWaves). The original algorithm used in Hobday et al. (2016) is available for use via python and may be found at https://github.com/ecjoliver/marineHeatWaves.

It is necessary to emphasise that MHWs as defined here exist against the daily climatological means of the time series in which they are found and not by exceeding an arbitrarily chosen static threshold. Therefore, one may just as likely find a MHW during winter months as summer months. This is a valuable characteristic of this method of investigation because aseasonal warm winter waters may have deleterious effects on relatively thermophobic species (Wernberg et al., 2011), while concurrently aiding the recruitment of con-specific species (cite).

2.5. Air-sea states

The synoptic air-sea state during each MHW was created by averaging the SST, air temperature, wind and current (U and V vectors) values from the BRAN and ERA-Interim products at a 0.5°resolution for each day found within the start and end date of each individual event for the entire study area. This allows for possible teleconnections between different coastal section to be incorporated into the study. An example output of one of the largest MHWs in the SACTN dataset may be seen in Figure 2. In order to create anomaly values for the synoptic states a daily climatology of the Julian day for each variable within each pixel was calculated using the same 11-day running mean used to determine seasonal climatologies for MHWs. This provided 366 mean air-sea states that could be subtracted from the daily air-sea values during a coastal MHW for the anomaly values.
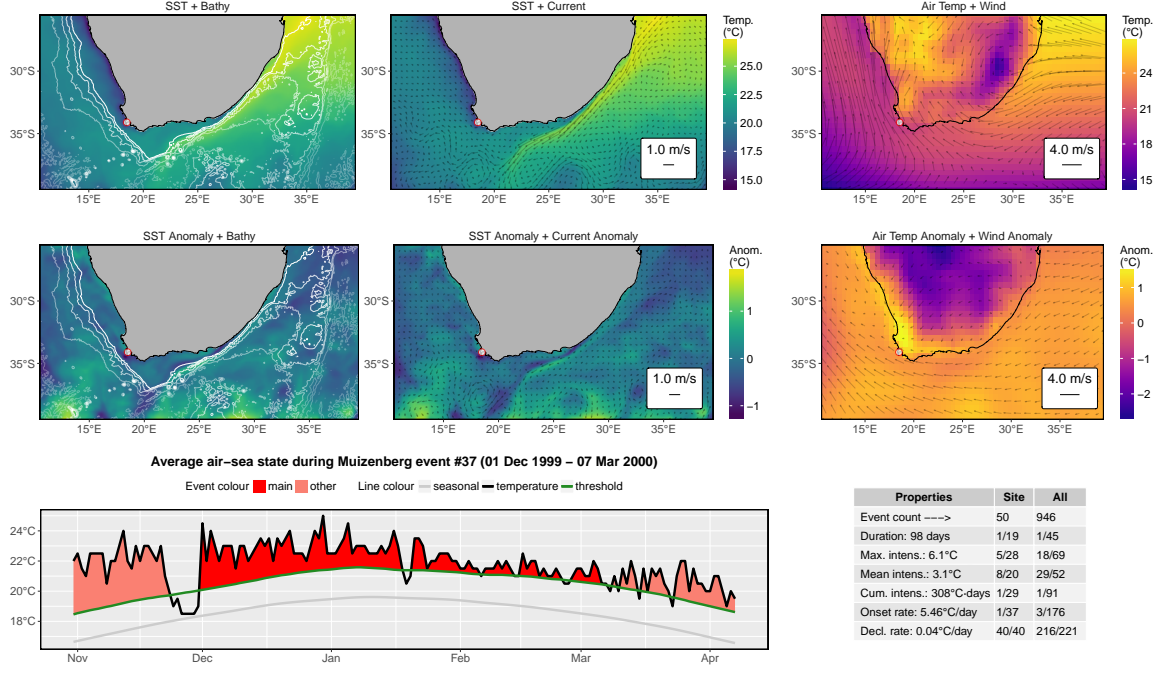
SST + Bathy | SST + Current | Air Temp + Wind

SST Anomaly + Bathy | SST Anomaly + Current Anomaly | Air Temp Anomaly + Wind Anomaly

Average air–sea state during Muizenberg event #37 (01 Dec 1999 – 07 Mar 2000)

Event colour ■ main ■ other   Line colour — seasonal — temperature — threshold

Properties	Site	All
Event count –––>	50	946
Duration: 98 days	1/19	1/45
Max. intens.: 6.1°C	5/28	18/69
Mean intens.: 3.1°C	8/20	29/52
Cum. intens.: 308°C-days	1/29	1/91
Onset rate: 5.46°C/day	1/37	3/176
Decl. rate: 0.04°C/day	40/40	216/221

Figure 2: Synoptic air and sea states during a marine heatwave (MHW).

¹⁷⁰ The daily anomalies during each of the 98 events for both air and sea states were meaned to create one mean air-sea state for each event. These synoptic air-sea states were them converted into single vectors with each pixel represented by one column. All 98 vectors representing each MHW were combined into one dataframe to allow for them to be used in a cluster analysis.

2.6. Cluster analysis

¹⁷⁵ There have been several methods employed in climate science to cluster synoptic air and or sea states. Most commonly in the past K-means clustering (Corte-Real et al., 1998; Burrough et al., 2001; Kumar et al., 2011, e.g.) or, to a lesser extent, hierarchical cluster analysis (HCA) (e.g. Unal et al., 2003) have been used. Though already decades old, the use of self-organising maps (SOMs) has been gaining in popularity in climate studies over only the past several years (e.g. Cavazos, 2000; Hewitson ¹⁸⁰ and Crane, 2002; Morioka et al., 2010). As it is outside of the focus of the research presented here, we will not go into detail on the differences in the results generated by the three aforementioned methods. We will state however that it was the SOMs that best clustered out the data when all methods were visualised in two dimensional via a principal component analysis (PCA). In addition to the superior pattern recognition displayed by the SOM method, the orientation of the nodes (clusters) as produced ¹⁸⁵ by the SOM is also of use to the interpretation of the results of this work.

The initialisation of a SOM is similar to more traditional clustering techniques in that K random points are chosen and from there the data points from the given dataset are re-oriented in an iterative process to reduce the within group sum of squares (Jain, 2010). SOMs differ from more traditional methods in that they also account for the stress of the clustered values in relation to one another and

7

endeavours to orient its nodes (clusters) into the least stressful position in two dimensional space. This allows one to further evaluate the relationship between the clustered air-sea states.

Because the synoptic air-sea states during each MHW consist of over 9,000 pixels it is difficult for a computer algorithm to arrive satisfactorily at a consistent answer each time the analysis is run. For this reason we opted out of using random initialization (RI) for our SOM models in favor of principal component initialization (PCI). PCI differs from RI in that it uses the two principal components of the dataset, as determined from a principal component analysis (PCA) to initialize the choice of node centers for the SOM. This allows the SOM model to create the exact same result whenever it is run on the same data.

The appropriate number of nodes (clusters) to use is always a contentious decision. We have chosen here to use 9 nodes for a number of reasons. The first reason was that SOMs are best run on even grids of data (e.g. 2x3, 3x3, 4x4, etc.) (cite). Because 4 nodes was too few, and 16 was too many, 9 was settled on as a provisional number. Calculating the within group sum of squares (WGSS) value as more nodes were included showed that 4 could be satisfactory, but that at least 6 would be better. By comparing the results of the PCA and hierarchical cluster analysis (HCA) also performed on these data (not included here) with the SOM results it became clear that 7 or more nodes (clusters) was appropriate. Ultimately we settled on 9 nodes as this allowed for a wider variety of different synoptic air-sea states to be separated out from one another, allowing for a better understanding of the dominant air-sea states that exist during coastal MHWs. A final consideration for the validity of the choice of nodes, as proposed in Johnson (2013), is that the nodes must be significantly different from one another. We found this to be true with a choice of 9 nodes.

Once each event was clustered into 1 of 9 nodes, the synoptic air-sea state for each node was calculated by taking the average for each pixel for each variable from all of the mean air-sea states for each MHW as outlined in the 'Air-sea states' section above. Ambroise et al. (2000) and Ramos (2001) provide examples for the use of multiple clustering techniques for categorizing climate data. We felt it was unnecessary to use more than one technique and so only use SOMs here.

3. Results

3.1. Air-sea states

The 9 most common air-sea states around southern Africa during coastal MHWs may be seen in Figure 3. The top nine panels show the SST and currents, while the bottom 9 panels show the air temperature and winds. All values shown are anomalies.

3.2. Nodes

Immediately apparent in the clustering of the data is that node 6 stands out in starkest contrast to the other nodes as containing the most anomalously warm air and sea as well as having the strongest winds. As one moves from the right hand nodes to the left they become progressively less anomalous. With less and less of a pattern present. These left hand nodes serve to show that there are still many
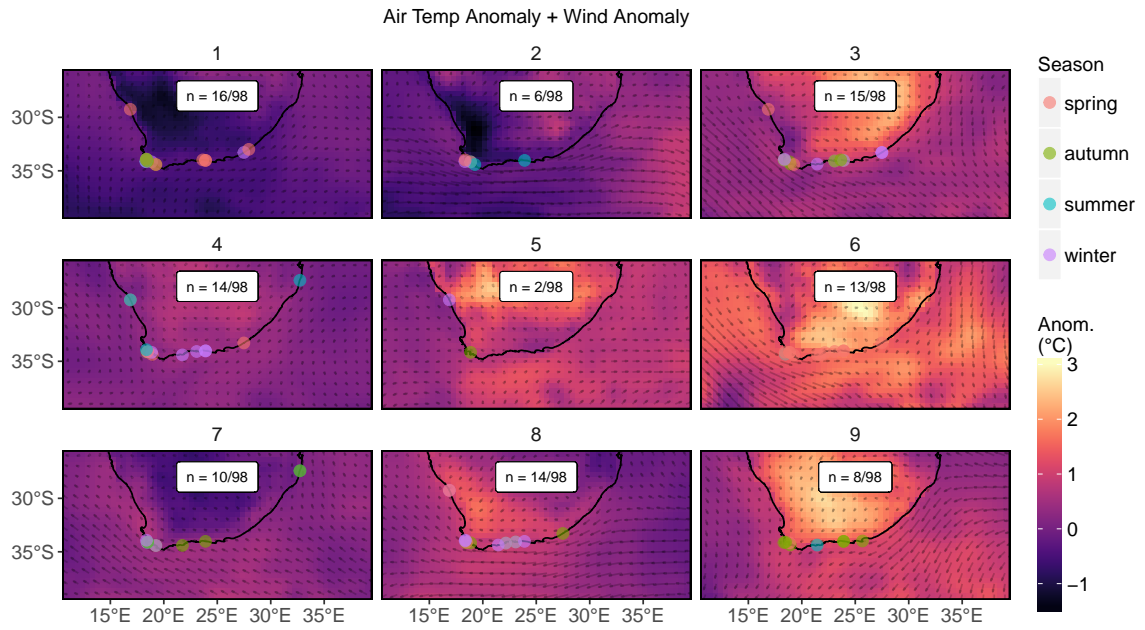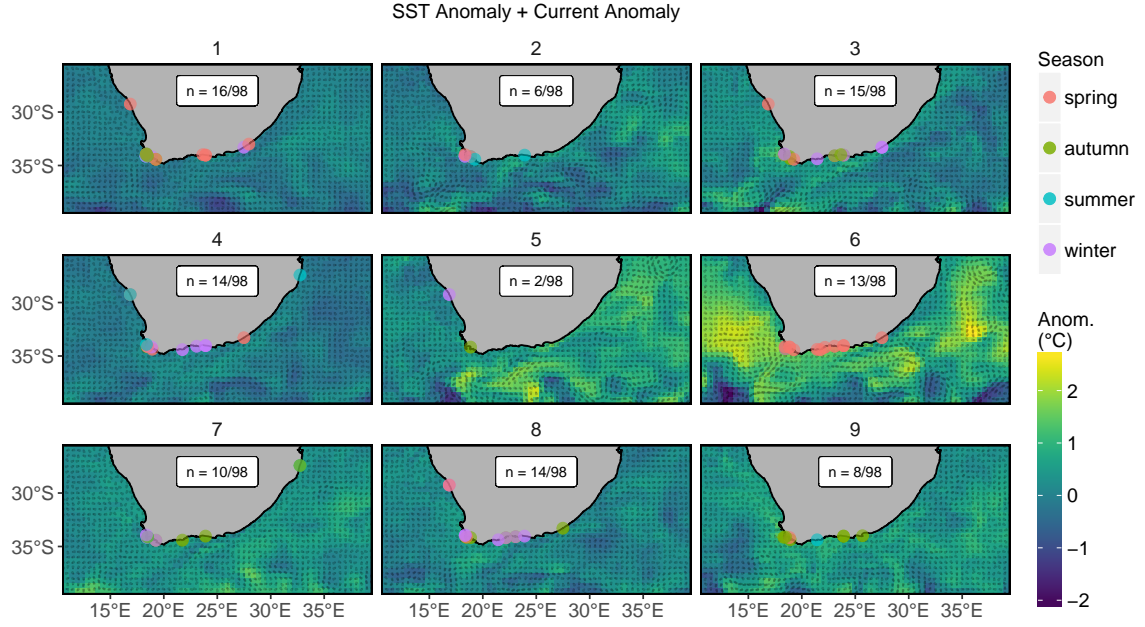
Figure 3: Common air and sea states during coastal marine heatwaves (MHWs).

coastal MHWs that occur without any apparent pattern. At least not a pattern that has occurred often enough over the past 30+ years that would afford them their own node. Due to the vast dissimilarity between the 9 nodes, only 2 events were clustered into the central node. Otherwise the clustering of events into nodes was equitable.

If we look at the events within the nodes via lolliplots (Figure 4) we see that only one of the nodes shows an air-sea state during primarily one large event that was recorded at multiple locations (node 6). Besides nodes 5 and 6, the other nodes consist of a medley of several independent events that occurred during different years and seasons, and of varying magnitudes, that cluster together due to their similarity. These nodes represent what a more common air-sea state during a coastal MHW may look like. Also important to note is that a common occurrence in all of the nodes, but particularly node 6, is the abnormal retroflection of the Agulhas current onto the Agulhas Bank.

3.3. Marine heatwaves

When we look at the statistics for each node (Table 2) we see that...

Table 2: The relevant metrics and statistics for the events found within each node.

	node	count	summer	autumn	winter	spring	west	south	east	duration_min	duration_mean	duration_max	int_cum_min	int_
1	1.00	16	2	4	3	7	7	8	1	15.00	22.20	43.00	24.49	
2	2.00	6	3	0	1	2	2	4	0	16.00	18.50	21.00	35.98	
3	3.00	15	0	6	7	2	4	11	0	15.00	23.70	48.00	23.77	
4	4.00	14	3	1	6	4	3	10	1	16.00	43.50	222.00	32.71	
5	5.00	2	0	1	1	0	1	1	0	19.00	42.00	65.00	70.44	
6	6.00	13	1	0	0	12	0	13	0	15.00	31.20	47.00	45.26	
7	7.00	10	2	5	3	0	1	7	2	16.00	30.00	98.00	20.57	
8	8.00	14	0	5	7	2	4	10	0	15.00	20.20	27.00	23.73	
9	9.00	8	1	6	0	1	1	7	0	15.00	17.50	21.00	28.74	
10		98	12	28	28	30	23	71	4	15.00	27.00	222.00	20.57	

4. Discussion

4.1. Abnormal behavior

Most notable from the clustering of these events has been the Agulhas current retroflecting north, rather than south, when coastal MHWs were detected. This is a similar finding to the cause of the Western Australia MHW (Feng et al., 2013; Benthuysen et al., 2014).

5. Conclusion

This research has highlighted that the cause of coastal MHWs is generally, but not always, due to the abnormal advection of water onto the coast due to meso-scale activity. In the case of the west and south coast sections of South Africa this offshore water is often warmer than coastal waters and so it was not necessary that the offshore waters be aseasonally warm at their point of origin. This finding shows that a knowledge of the meso-scale oceanographic properties of an area is necessary to determine what forces may be causing MHWs along a stretch of coastline. Once these areas have been identified, it may then be possible to develop a warning system given a threshold of days during which anomalous currents may be found along a coastline.
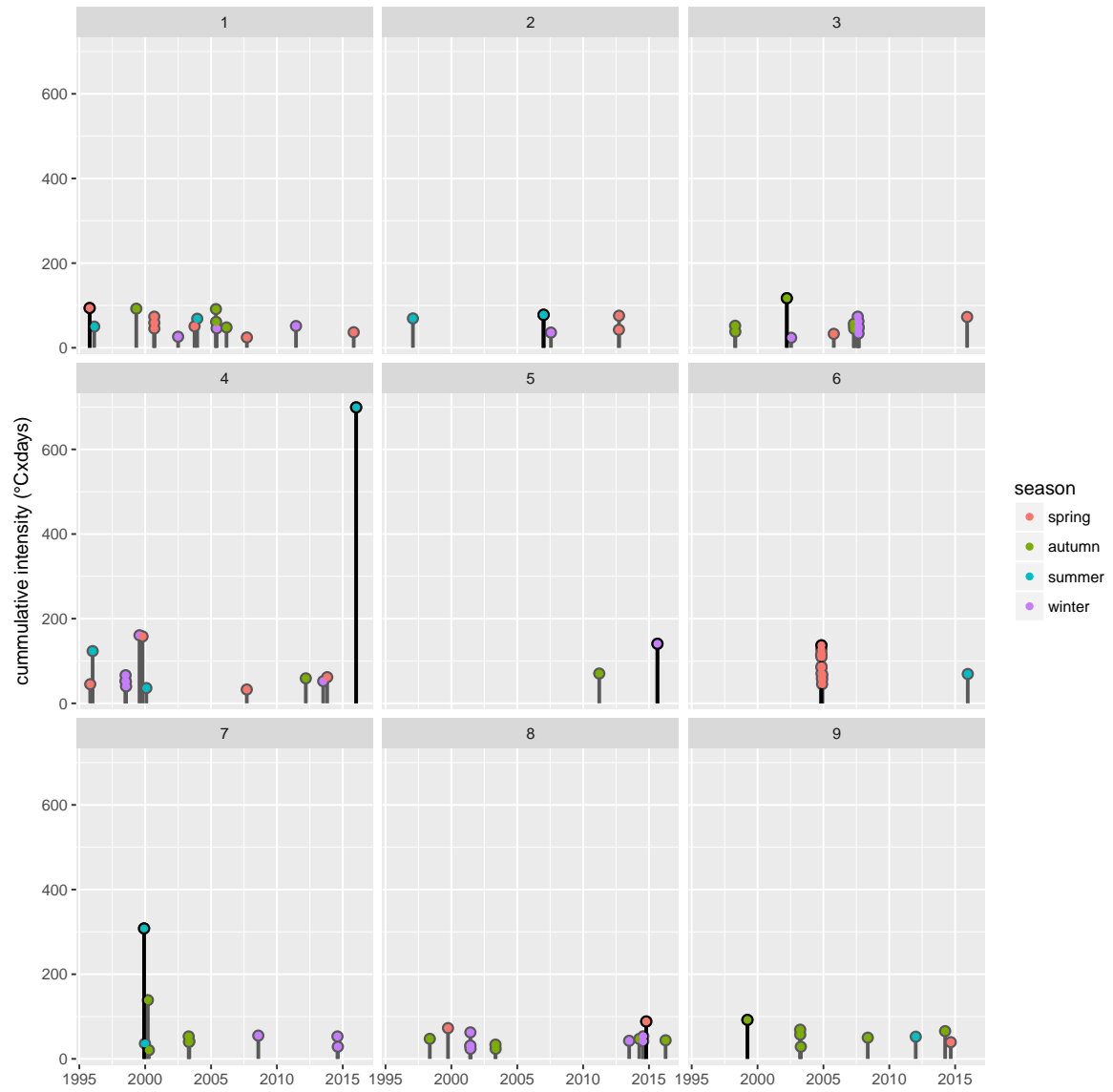
Figure 4: Lolliplot showing the date during which each event began. The height of each lolli shows the cumulative intensity of the event for comparison of the severity of the events.

Table 3: The metadata and coastal averages for all *in situ* time series used in this study.

	order	site	src	index	lon	lat	depth	type	coast	date.start	date.end	length	N.
84	2	Port Nolloth	SAWS	Port Nolloth/ SAWS	16.87	-29.25	0	thermo	wc	1299.00	16800.00	15502	
100	16	Sea Point	SAWS	Sea Point/ SAWS	18.38	-33.92	0	thermo	wc	1461.00	16527.00	15067	
71	17	Oudekraal	DAFF	Oudekraal/ DAFF	18.35	-33.98	9	UTR	wc	12108.00	16835.00	4728	
41	18	Hout Bay	DEA	Hout Bay/ DEA	18.35	-34.05	28	UTR	wc	7753.00	13992.00	6240	
52	20	Kommetjie	SAWS	Kommetjie/ SAWS	18.33	-34.14	0	thermo	wc	8095.00	16527.00	8433	
12	22	Bordjies	DAFF	Bordjies/ DAFF	18.46	-34.32	4	UTR	sc	12502.00	16748.00	4247	
13	23	Bordjies Deep	DAFF	Bordjies Deep/ DAFF	18.47	-34.31	9	UTR	sc	12087.00	16748.00	4662	
33	27	Fish Hoek	SAWS	Fish Hoek/ SAWS	18.44	-34.14	0	thermo	sc	8095.00	16527.00	8433	
65	29	Muizenberg	SAWS	Muizenberg/ SAWS	18.48	-34.10	0	thermo	sc	1220.00	16527.00	15308	
36	30	Gordons Bay	SAWS	Gordons Bay/ SAWS	18.86	-34.16	0	thermo	sc	986.00	16527.00	15542	
10	31	Betty's Bay	DAFF	Betty's Bay/ DAFF	18.92	-34.36	5	UTR	sc	12765.00	16751.00	3987	
38	32	Hermanus	SAWS	Hermanus/ SAWS	19.25	-34.41	0	thermo	sc	7274.00	16527.00	9254	
109	37	Stilbaai	SAWS	Stilbaai/ SAWS	21.44	-34.37	0	thermo	sc	3652.00	16527.00	12876	
131	38	Ystervarkpunt	DEA	Ystervarkpunt/ DEA	21.74	-34.40	3	UTR	sc	9426.00	13685.00	4260	
61	39	Mossel Bay	DEA	Mossel Bay/ DEA	22.16	-34.18	8	UTR	sc	7846.00	13685.00	5840	
50	42	Knysna	DEA	Knysna/ DEA	23.07	-34.08	7	UTR	sc	9210.00	14554.00	5345	
119	45	Tsitsikamma West	SAWS	Tsitsikamma/ SAWS	23.65	-33.98	0	thermo	sc	7486.00	13559.00	6074	
111	46	Storms River Mouth	SAWS	Storms River Mouth/ SAWS	23.90	-34.02	0	thermo	sc	8491.00	14244.00	5754	
118	47	Tsitsikamma East	DEA	Tsitsikamma/ DEA	23.91	-34.03	10	UTR	sc	7849.00	14558.00	6710	
78	58	Pollock Beach	SAWS	Pollock Beach/ SAWS	25.68	-33.99	0	thermo	sc	10724.00	16527.00	5804	
43	59	Humewood	SAWS	Humewood/ SAWS	25.65	-33.97	0	thermo	sc	1332.00	10956.00	9625	
37	67	Hamburg	DEA	Hamburg/ DEA	27.49	-33.29	4	UTR	sc	9433.00	14667.00	5235	
30	68	Eastern Beach	SAWS	Eastern Beach/ SAWS	27.92	-33.02	0	thermo	ec	5113.00	10438.00	5326	
70	69	Orient Beach	SAWS	Orient Beach/ SAWS	27.92	-33.02	0	thermo	ec	5113.00	16527.00	11415	
68	70	Nahoon Beach	SAWS	Nahoon Beach/ SAWS	27.95	-32.99	0	thermo	ec	5113.00	10438.00	5326	
102	133	Sodwana	DEA	Sodwana/ DEA	32.73	-27.42	18	UTR	ec	8835.00	14636.00	5802	

Acknowledgements

Supplementary

Meta-data

Further meta-data for each time series and source listed in geographic order along the South African coast from the border of Namibia to the border of Mozambique may be found in Table 3.

References

Ambroise, C., S??ze, G., Badran, F., Thiria, S., 2000. Hierarchical clustering of self-organizing maps for cloud classification. Neurocomputing 30 (1-4), 47–52.

Barsugli, J. J., Battisti, D. S., 1998. The Basic Effects of Atmosphere–Ocean Thermal Coupling on Midlatitude Variability*. Journal of the Atmospheric Sciences 55 (4), 477–493.

Benthuysen, J., Feng, M., Zhong, L., 2014. Spatial patterns of warming off Western Australia during the 2011 Ningaloo Niño: quantifying impacts of remote and local forcing. Continental Shelf Research 91, 232–246.

Burrough, P. A., Wilson, J. P., Van Gaans, P. F. M., Hansen, A. J., 2001. Fuzzy k-means classification of topo-climatic data as an aid to forest mapping in the Greater Yellowstone Area, USA. Landscape Ecology 16 (6), 523–546.

Castillo, K. D., Lima, F. P., 2010. Comparison of in situ and satellite-derived (MODIS-Aqua/Terra) methods for assessing temperatures on coral reefs. Limnology and Oceanography Methods 8, 107–117.

Cavazos, T., 2000. Using self-organizing maps to investigate extreme climate events: An application to wintertime precipitation in the Balkans. Journal of Climate 13 (10), 1718–1732.

Corte-Real, J., Qian, B., Xu, H., 1998. Regional climate change in Portugal: precipitation variability associated with large-scale atmospheric circulation. International Journal of Climatology 18 (6), 619–635.
URL   http://onlinelibrary.wiley.com/doi/10.1002/(SICI)1097-0088(199805)18: 6{%}3C619::AID-JOC271{%}3E3.0.CO;2-T/abstracthttp://www.scopus.com/scopus/inward/ record.url?eid=2-s2.0-3543007704{&}partnerID=40{&}rel=R7.0.0

Deser, C., Alexander, M. A., Xie, S. P., Phillips, A. S., 2010. Sea surface temperature variability: patterns and mechanisms. Annual Review of Marine Science 2, 115–143.

Easterling, D. R., Meehl, G. A., Parmesan, C., Changnon, S. A., Karl, T. R., Mearns, L. O., 2000. Climate extremes: observations, modeling, and impacts. Science 289 (5487), 2068–2074.

Feng, M., McPhaden, M. J., Xie, S.-P., Hafner, J., 2013. La Niña forces unprecedented Leeuwin Current warming in 2011. Scientific Reports 3, 1277.

Frankignoul, C., 1985. Sea surface temperature anomalies, planetary waves, and air-sea feedback in the middle latitudes.

Garrabou, J., Coma, R., Bensoussan, N., Bally, M., Chevaldonné, P., Cigliano, M., Diaz, D., Harmelin, J. G., Gambi, M. C., Kersting, D. K., Ledoux, J. B., Lejeusne, C., Linares, C., Marschal, C., Pérez, T., Ribes, M., Romano, J. C., Serrano, E., Teixido, N., Torrents, O., Zabala, M., Zuberer, F., Cerrano, C., 2009. Mass mortality in Northwestern Mediterranean rocky benthic communities: effects of the 2003 heat wave. Global Change Biology 15 (5), 1090–1103.

Hewitson, B. C., Crane, R. G., 2002. Self-organizing maps: Applications to synoptic climatology. Climate Research 22 (1), 13–26.

Hobday, A. J., Alexander, L. V., Perkins, S. E., Smale, D. A., Straub, S. C., Oliver, E. C., Benthuysen, J. A., Burrows, M. T., Donat, M. G., Feng, M., Holbrook, N. J., Moore, P. J., Scannell, H. A., Sen Gupta, A., Wernberg, T., 2016. A hierarchical approach to defining marine heatwaves. Progress in Oceanography 141, 227–238.

Hutchings, L., van der Lingen, C. D., Shannon, L. J., Crawford, R. J. M., Verheye, H. M. S., Bartholomae, C. H., van der Plas, a. K., Louw, D., Kreiner, A., Ostrowski, M., Fidel, Q., Barlow, R. G., Lamont, T., Coetzee, J., Shillington, F., Veitch, J., Currie, J. C., Monteiro, P. M. S., 2009. The Benguela Current: an ecosystem of four components. Progress in Oceanography 83 (1-4), 15–32.

Jain, A. K., 2010. Data clustering: 50 years beyond K-means. Pattern Recognition Letters 31 (8), 651–666.

Jentsch, A., Kreyling, J., Beierkuhnlein, C., 2007. A new generation of climate-change experiments: events, not trends. Frontiers in Ecology and the Environment 5 (6), 315–324.

Johnson, N. C., 2013. How many enso flavors can we distinguish? Journal of Climate 26 (13), 4816–4827.

Krishnamurti, T. N., Oosterhof, D. K., Mehta, A. V., 1988. Air–Sea Interaction on the Time Scale of 30 to 50 Days.
URL `http://dx.doi.org/10.1175/1520-0469(1988)045{%}3C1304:AIOTTS{%}3E2.0.CO;2`

Kumar, J., Mills, R. T., Hoffman, F. M., Hargrove, W. W., 2011. Parallel k-means clustering for quantitative ecoregion delineation using large data sets. In: Procedia Computer Science. Vol. 4. pp. 1602–1611.

Lünning, K., 1990. Seaweds: their environment, biogeography and ecophysiology. John Wiley and Sons. Wiley, New York (USA).

Morioka, Y., Tozuka, T., Yamagata, T., 2010. Climate variability in the southern Indian Ocean as revealed by self-organizing maps. Climate Dynamics 35 (6), 1075–1088.

Perkins, S. E., Alexander, L. V., 2013. On the measurement of heat waves. Journal of Climate 26 (13), 4500–4517.

Ramos, M. C., 2001. Divisive and hierarchical clustering techniques to analyse variability of rainfall distribution patterns in a Mediterranean region. Atmospheric Research 57 (2), 123–138.

Schlegel, R. W., Smit, A. J., 2016. Climate Change in Coastal Waters: Time Series Properties Affecting Trend Estimation. Journal of Climate 29 (24), 9113–9124.
URL `http://journals.ametsoc.org/doi/10.1175/JCLI-D-16-0014.1`

Smale, D. A., Wernberg, T., 2009. Satellite-derived SST data as a proxy for water temperature in nearshore benthic ecology Peer reviewed article. Marine Biology 387, 27–37.

Smit, A. J., Roberts, M., Anderson, R. J., Dufois, F., Dudley, S. F. J., Bornman, T. G., Olbers, J., Bolton, J. J., 2013. A coastal seawater temperature dataset for biogeographical studies: large biases between in situ and remotely-sensed data sets around the coast of South Africa. PLOS ONE 8 (12).

Stocker, T., Qin, D., Plattner, G. K., Tignor, M., Allen, S. K., Boschung, J., Nauels, A., Xia, Y., Bex, V., Midgley, P. M. (Eds.), 2013. Climate change 2013: the physical science basis: Working Group I contribution to the Fifth Assessment Report of the Intergovernmental Panel on Climate Change. Cambridge University Press, Cambridge, United Kingdom and New York, NY, USA.

Unal, Y., Kindap, T., Karaca, M., 2003. Redefining the climate zones of Turkey using cluster analysis. International Journal of Climatology 23 (9), 1045–1055.

Wernberg, T., Bennett, S., Babcock, R. C., Bettignies, T. D., Cure, K., Depczynski, M., Dufois, F., Fromont, J., Fulton, C. J., Hovey, R. K., Harvey, E. S., Holmes, T. H., Kendrick, G. A., Radford, B., Santana-garcon, J., Saunders, B. J., Smale, D. A., Thomsen, M. S., 2016. Climate driven regime shift of a temperate marine ecosystem. Science 149 (1996), 2009–2012.

Wernberg, T., Russell, B. D., Moore, P. J., Ling, S. D., Smale, D. A., Campbell, A., Coleman, M. A., Steinberg, P. D., Kendrick, G. A., Connell, S. D., 2011. Impacts of climate change in a global hotspot for temperate marine biodiversity and ocean warming. Journal of Experimental Marine Biology and Ecology 400 (1-2), 7–16.